Journal of Achievements in Materials and Manufacturing Engineering
VOLUME 37
ISSUE 2
December
2009

Microstructures in $Fe_{30}Ni_{30}Cu_{20}P_{10}Si_5B_5$ melt-spun alloy ejected at various temperatures

K. Ziewiec [a,*], A. Ziewiec [b], K. Prusik [c]
[a] Pedagogical University of Cracow, ul. Podchorążych 2, 30-084 Kraków, Poland
[b] Faculty of Metallurgy and Materials Science, University of Mining and Metallurgy, Al. Mickiewicza 30, 30-059 Kraków, Poland
[c] Institute of Material Science, University of Silesia, ul. Bankowa 12, 40-007 Katowice, Poland
* Corresponding author: E-mail address: kziewiec@ap.krakow.pl

Received 21.09.2009; published in revised form 01.12.2009

Properties

ABSTRACT

Purpose: The aim of the work is to study the influence of ejection temperature on the structure of $Fe_{30}Ni_{30}Cu_{20}P_{10}Si_5B_5$ melt-spun.

Design/methodology/approach: A six-component $Fe_{30}Ni_{30}Cu_{20}P_{10}Si_5B_5$ alloy was arc-melt in argon protective atmosphere from of pure Fe, Ni, Cu elements and Fe-P, Fe-B, Ni-P, Ni-B master alloys and melt-spun in helium. The alloy was melt-spun in various temperatures. Morphology and chemical composition of the cross-section of the ingot and melt-spun ribbons were analysed with scanning electron microscope SEM with energy dispersive spectrometer EDS. The melt-spun ribbon was investigated by means of the transmission electron microscope (TEM). The melting range of the alloy was investigated by means of differential thermal analysis at the heating rate 20 K/min.

Findings: The slow cooling rate resulted in the fractal-like structures formed by the Fe-rich regions and Cu-rich regions typical for the alloying system with a miscibility gap. The structures observed after rapid cooling were dependent on ejection temperatures of the alloy just before the melt spinning process. The lower ejection temperatures led to the formation of crystalline structures separated into Fe-rich and Cu-rich regions which were a result of rapid cooling within the miscibility gap. The higher ejection temperatures contributed to formation of amorphous/crystalline composite. The crystalline spherical precipitates were found to be predominantly Cu-base solid solution.

Research limitations/implications: It has been shown that the multi-component Fe-Ni-Cu-P-Si-B alloy provides possibility of microstructure control of amorphous/crystalline composite due to miscibility gap.

Practical implications: The work reports that the ductile phase can be introduced into the amorphous alloy by using a suitable ejection temperature control in a melt spinning process, providing possibility of controlling properties in glassy matrix alloys.

Originality/value: The study provides original information about the primary structure of the arc-melt $Fe_{30}Ni_{30}Cu_{20}P_{10}Si_5B_5$ alloy as well as about the microstructure of melt-spun alloy using various ejection temperatures.

Keywords: Amorphous/crystalline composites; Miscibility gap; Arc melting; Melt spinning

Reference to this paper should be given in the following way:
K. Ziewiec, A. Ziewiec, K. Prusik, Microstructures in $Fe_{30}Ni_{30}Cu_{20}P_{10}Si_5B_5$ melt-spun alloy ejected at various temperatures, Journal of Achievements in Materials and Manufacturing Engineering 37/2 (2009) 532-537.

1. Introduction

Entirely amorphous metallic structure generally presents superior properties in comparison with the traditional crystalline alloys. They are attractive due to their high strength, high elastic limit and soft magnetism [1-5]. Nevertheless, for some applications, it would be useful to produce a composite material, joining the properties of the amorphous matrix and a highly dispersed fine crystalline phase [6]. This could be potentially useful in such cases as improving ductility by introducing a soft crystalline phase or increasing coercivity in hard magnet structures with use of a paramagnetic phase. Such works have already been made in order to improve the ductility by means of ductile crystalline phase formed in situ [7, 8]. Alternatively, the composites can be formed by introducing the particles ex situ prior to casting [7-9], or by formation of the crystalline phase in situ. The latter can be carried out by crystallization of the amorphous matrix or the formation of the crystalline phase during casting [10-14]. The formation of primary dendritic crystals may not be effective as their formation sometimes is suppressed due to the existence of the eutectic zone. Another idea to form a composite is using an immiscible alloy system. Production of the composite directly from the liquid state, using miscibility gap is justified as regards energy saving because no additional heat treatment to produce the fine crystalline phase is necessary. So far, there have been reports on formation of two-phased glassy composites in Ni-Nb-Y system [15, 16], Y-Ti-Al-Co system [17]. As regards the iron based alloys, it can be found that glass formation is possible in iron metalloid ternary Fe-Si-P, Fe-Si-B, Fe-P-B, Fe-Ni-P, Fe-Ni-B systems [18]. On the other hand, Fe-Cu-P, Fe-Cu-Si, Fe-Cu-B systems have a miscibility gap in the liquid phase [19], therefore we considered the Fe-Cu-Ni-P-Si-B system for experiment. In order to forecast the behaviour of the multi-component system it is useful to know the enthalpies of mixing in liquid binary systems [20, 21] (see Table 1).

The Fe-Cu-Ni-P-Si-B system will probably show a tendency to separate into Fe-rich and Cu-rich regions due to a positive enthalpy of mixing between iron and copper as it is observed in ternary Fe-Cu-P, Fe-Cu-Si [19]. On the other hand, relatively highly negative enthalpy of mixing for iron and nickel with P, Si and B as well as nickel and copper with phosphorus may facilitate the amorphization of the alloy. Therefore, the aim of the work is to study the effects of mixing the above mentioned elements in the $Fe_{30}Ni_{30}Cu_{20}P_{10}Si_5B_5$ alloy in order to make the amorphous/crystalline composite.

2. Experimental

The $Fe_{30}Ni_{30}Cu_{20}P_{10}Si_5B_5$ alloy was prepared by arc melting of pure elements 99.95 wt. % Ni, 99.95 wt. % Cu, 99.95 wt. % Fe, 99.999 wt. % Si and Fe-P, Fe-B, Ni-P, Ni-B master alloys. The alloy was melted 5 times under titanium gettered argon atmosphere. Morphology and chemical composition of the cross-section of the ingot were analysed with scanning electron microscope (SEM) Philips XL 30 with X-Ray microanalyses Link ISIS-EDX. The alloy was melt-spun in helium atmosphere with the linear velocity of 33 m/s, ejection pressure 150 kPa, crucible and hole diameter 0.7 mm starting from different temperatures i.e.: 1273 K, 1400 K, 1509 K, 1560 K where the pouring temperature was controlled using RAYTECH MARATHON series BH2MR1SBSF two-colour pyrometer. The microstructure of the melt-spun ribbons was investigated by means of scanning electron microscope (SEM) Philips XL 30 with X-Ray microanalyses Link ISIS-EDX and by means of the JEOL 300 kV transmission electron microscope (TEM). The alloy was also investigated by means of differential thermal analysis (DTA-STD 2960 TA Instruments) at the heating rate 20 K/min.

3. Results

The results of microstructure SEM/EDS examination of the arc melted droplet are presented on Fig. 1. The surface fractal [22] morphology of the alloy consists of the bright globular regions marked “A” within the darker matrix marked “B”.

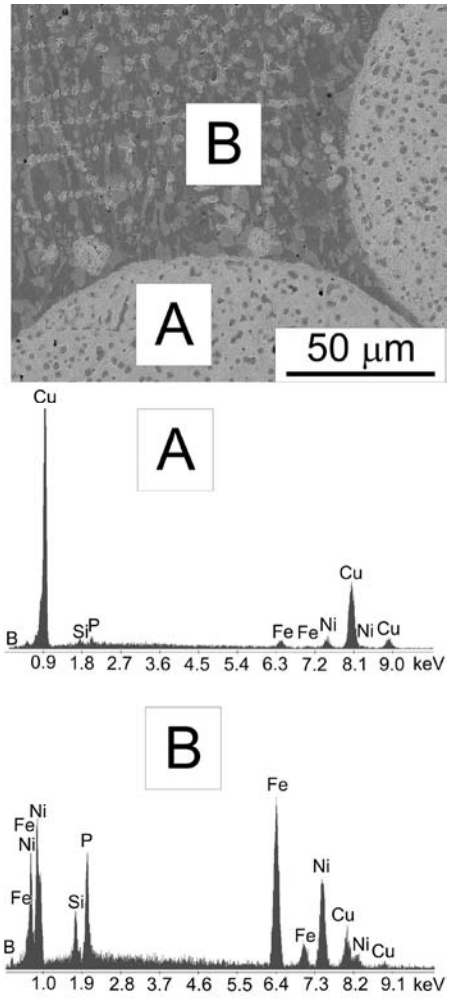

Fig. 1. SEM image of the arc-melt $Fe_{30}Ni_{30}Cu_{20}P_{10}Si_5B_5$ alloy and EDS analysis for regions A and B

Regions "A" are enriched with copper and rather impoverished in the other chemical constituents. There are only small EDS peaks for Fe, Ni, P, Si and B. The above mentioned elements are mainly located in Fe-reach matrix. As regards boron, here are only small peaks present in both Cu-based and Fe-based regions, however it can be expected that due to negative mixing enthalpy for Fe-B (-11 kJ/mol) and positive one for Cu-B (+16 kJ/mol) (Table 1) boron will be strongly attracted in iron-rich "B" regions. Therefore, before solidification, the Fe-rich liquid matrix, regions "B", were also enriched with nickel, phosphorus, silicon and probably boron.

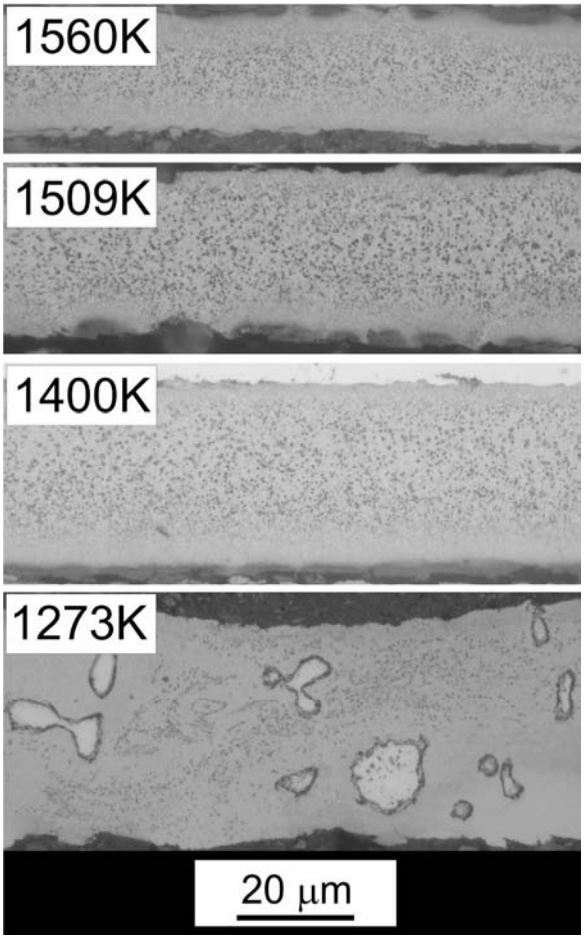

Fig. 2. Light microscope images of $Fe_{30}Ni_{30}Cu_{20}P_{10}Si_5B_5$ melt spun ribbons from different ejection temperatures

Table 1.
Calculated enthalpies of mixing for equiatomic liquids in binary systems for, kJ/mol [20, 21*]

	Fe	Cu	Ni	P	Si	B
Fe	-	+13.0	-2.0	-31.0	-18.0	-11.0
Cu		-	+4.0	-17.5	-10.0	+16.0*
Ni			-	-26.0	-23.0	-9.0

* Mixing enthalpy for Cu-B is approximated based on [21]

The light microphotographs of the ribbons, melt-spun starting from the different melt temperatures are shown in Fig. 2. For 1273 K the appearance of the cross-section is inhomogeneous. It is possible to observe relatively large copper-base globular regions of a few microns size. For the ribbon cast from 1273 K (Fig. 3), the tendency for segregation of chemical elements is similar as in case of as-cast of the arc melt droplet, i.e. we observe copper-rich precipitates and iron-rich matrix. Copper-rich regions are also impoverished in nickel, phosphorus, and probably in boron. However, distribution of silicon is apparently uniform. For the higher temperatures i.e.: 1400 K, 1509 K, 1560 K homogeneous structure of the ribbon with fine particles was obtained and TEM observations revealed particles of the average size of generally lower than 100nm within amorphous matrix. Electron diffraction patterns show broad diffusive rings typical for the amorphous structure (Fig. 4). Majority of the spherical particles could be identified as Cu-base (Fm-3m).

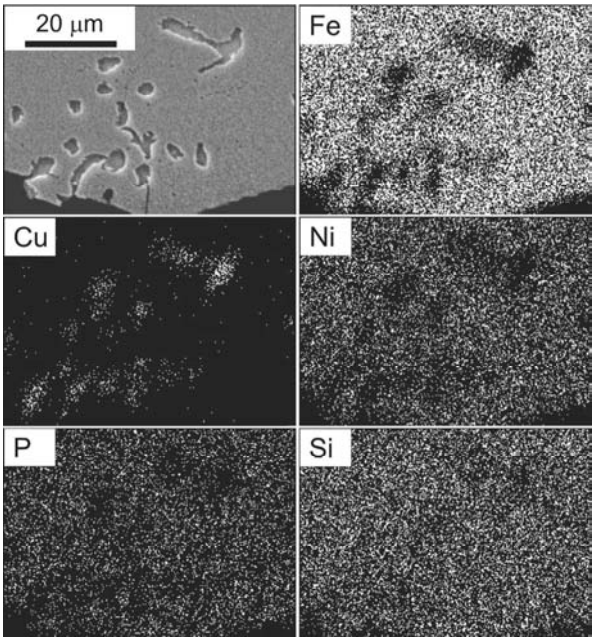

Fig. 3. Cross section SEM image with mapping of elements for $Fe_{30}Ni_{30}Cu_{20}P_{10}Si_5B_5$ melt-spun ribbon ejected at 1273 K

DTA run of the $Fe_{30}Ni_{30}Cu_{20}P_{10}Si_5B_5$ alloy is presented on Fig. 5. Melting of the alloy occurs in a two-step sequence with the beginning at T_m=1164 K and the end at T_m=1242 K. The end-set of the miscibility region can be observed at T_c=1315 K occurring probably due to dissolution of melts that were insoluble at lower temperatures. In the binary monotectic alloys the transformation from crystalline state to a uniform liquid phase may follow as a result of a multi-step reaction including as many as four stages, i.e.: melting of eutectics (peritectics), dissolution in the liquid of off-eutectic crystals, monotectic reaction, and mutual dissolution of insoluble liquids.

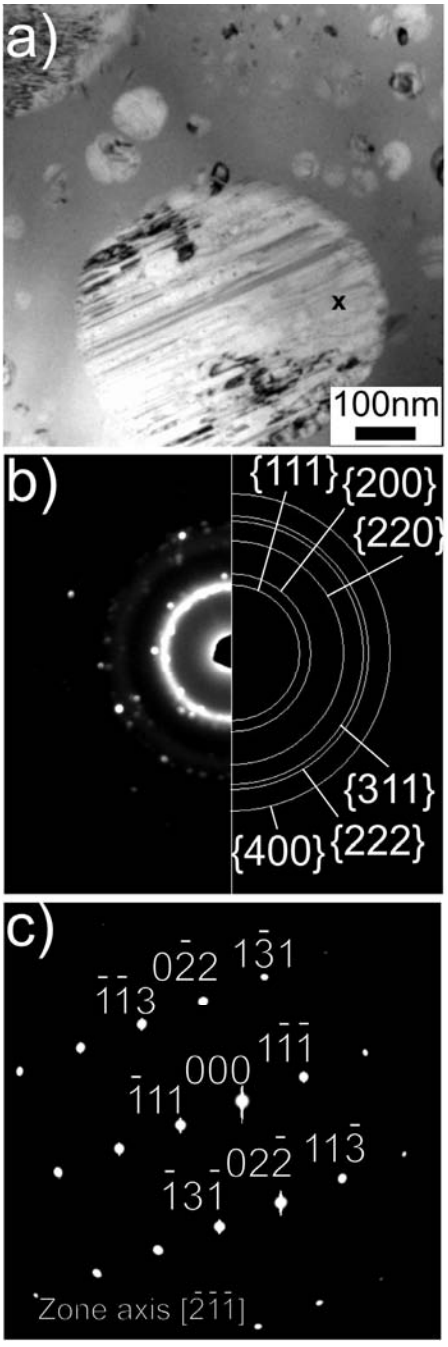

Fig. 4. TEM image of the $Fe_{30}Ni_{30}Cu_{20}P_{10}Si_5B_5$ melt spun ribbon ejected at 1560K; a) surface fractal microstructure; b) ring diffraction pattern for an extensive area with a broad diffusive ring from the amorphous matrix, rings and dot patterns for Cu-base fcc phase (Fm-3m); c) diffraction of the large spherulitic particle marked with "x"

Formation of the surface fractal structure is observed, which is typical for the systems with a miscibility gap [22]. As the cooling rate after the arc melting is relatively slow (order of 100 K/s), even the alloy with the initial temperature assuring a single homogeneous liquid will separate into two liquids, and then those melts will separate into the range of compositions depending on the slope of the miscibility gap curve. This can finally develop the fractal-like structure with a quite substantial scatter of sizes (e.g.: from a few mm to a few μm) and it was found in the arc-melt sample. However, in case of the $Fe_{30}Ni_{30}Cu_{20}P_{10}Si_5B_5$ melt-spun ribbons different structures can be observed. For the melt spinning at lower temperatures, separation in the liquid state produced Fe-rich regions and Cu-rich regions and the spatial distribution was inhomogeneous, similarly as in arc melt sample. The melt spinning technique caused mainly by grain refinement of Cu-rich regions (Fig. 2 and Fig. 3). However, increasing the melt spinning temperature to values as high as 1400 K causes homogenization of the structure visible on light micrographs of the samples ejected at 1400 K, 1509 K and 1560 K (Fig. 2).

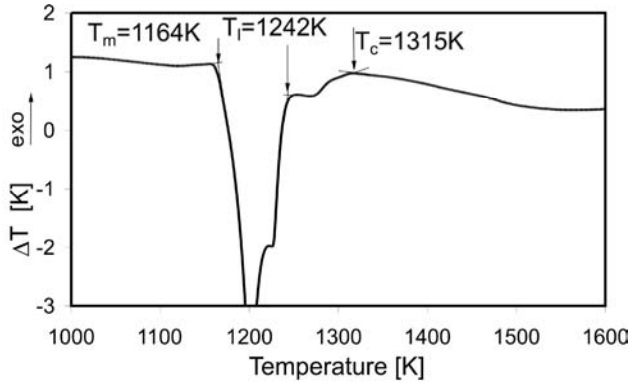

Fig. 5. DTA curve of the $Fe_{30}Ni_{30}Cu_{20}P_{10}Si_5B_5$ alloy

The uniform distribution found in these ribbons in contrast to the non-uniform structure obtained after ejection from lower temperatures, can be explained by the fact that in the former case the alloy was cast from homogenous melt above the miscibility gap in the system. The similar observation was found also in Fe-Cu-Si-B-Al-Ni-Y alloys [23].

As it is found from DTA curve, the alloy melts between T_m=1164 K and T_l=1242 K. However, there is a temperature range, where non-uniform structure after melt spinning can be obtained. This corresponds, probably to the miscibility gap for the $Fe_{30}Ni_{30}Cu_{20}P_{10}Si_5B_5$ alloy, found between T_l=1242 K and T_c=1315 K as an endothermic effect [24, 25]. Thus, after dissolution of the liquids, one liquid provides the uniform structure of the ribbons during the melt spinning. The sequence of existence of insoluble liquids "L_1+L_2", and uniform liquid "L" as well as the temperatures of ejection before the melt spinning marked with (●) is presented in Fig. 6. In comparison with the ternary Fe-Cu-P system [19], where the miscibility region seems to be very extensive (from c.a. 1300 K to at least 1600 K), the $Fe_{30}Ni_{30}Cu_{20}P_{10}Si_5B_5$ alloy was prepared by partial substitution of iron with nickel and phosphorus with silicon and boron. As a result, a substantially lower melting range T_l-T_m as well as a narrower miscibility gap (Fig. 5) in comparison with the Fe-Cu-P system was obtained.

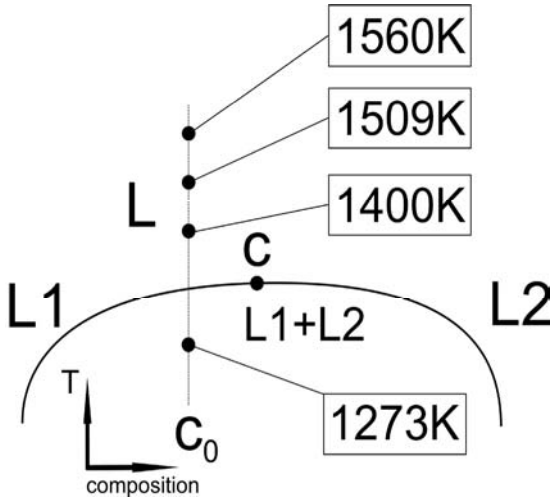

Fig. 6. Schematic temperature-composition diagram with the regions of insoluble liquids (L1+L2) and regions of the homogeneous liquids; "c" - critical point; "c_0" - nominal composition; the various ejection temperatures are marked with (•)

4. Conclusions

1. The arc-melt ingot microstructure of the $Fe_{30}Ni_{30}Cu_{20}P_{10}Si_5B_5$ alloy after a relatively slow cooling (10^2K/s) has the fractal-like morphology formed as a result of separation of liquids.
2. The arc-melt microstructure consists of the Fe-rich matrix and spherical Cu-rich regions. The Fe-rich regions are highly alloyed than Cu-rich regions. Silicon has the most uniform distribution between the Fe-rich and Cu-rich colonies. Formation of such regions is in agreement with expectations based on the enthalpies of mixing between the pairs of the alloying constituents.
3. The microstructure of the melt-spun alloy depends on ejection temperature before the melt spinning process. Low ejection temperature favours formation of a non-uniform crystalline structure where Fe-rich matrix and Cu-rich regions of a few μm are observed. This is probably due to the ejection within the miscibility gap between T_l=1242K and T_c=1315K. Higher ejection temperatures resulted from formation of uniform structure of the ribbon in the scale of a light microscope. This corresponds to the region of a uniform liquid above the miscibility gap.
4. Higher ejection temperatures of the melt spinning process (i.e. 1400K and more) resulted from the formation of very fine spherical particles uniformly distributed in an amorphous matrix. The spherical precipitates were crystalline and generally consisted of Cu-base solid solution.
5. Alloying of the simple ternary immiscible Fe-Cu-P system with Ni, Si and B provides substantially lower range of melting temperatures, decreasing and narrowing the miscibility gap.

References

[1] H. Warlimont, Amorphous metals driving materials and process innovations, Materials Science and Engineering A304-306 (2001) 61-67.
[2] A. Makino, T. Hatanai, A. Inoue, T. Masumoto, Nanocrystalline soft magnetic Fe-M-B (M = Zr, Hf, Nb) alloys and their applications, Materials Science and Engineering A226-228 (1997) 594-602.
[3] T. Kulik, Nanocrystallization of metallic glasses, Journal of Non-Crystalline Solids 287 (2001) 145-161.
[4] B. Kostrubiec, R. Wiśniewski, J. Rasek, Crystallisation kinetics and magnetic properties of a Co-based amorphous alloy, Journal of Achievements in Materials and Manufacturing Engineering 16 (2006) 30-34.
[5] S. Lesz, D. Szewieczek, J.E. Frąckowiak, Structure and magnetic properties of amorphous and nanocrystalline $Fe_{85.4}Hf_{1.4}B_{13.2}$ alloy, Journal of Achievements in Materials and Manufacturing Engineering 19/2 (2006) 29-34.
[6] K. Ziewiec, K. Bryła, A. Ziewiec, K. Prusik, The microstructure and properties of a new $Fe_{41}Ni_{39}P_{10}Si_5B_5$ glass forming alloy, Archives of Materials Science and Engineering 34/1 (2008) 35-38.
[7] S.W. Lee, M.Y. Huh, E. Fleury, J.C. Lee, Crystallization-induced plasticity of Cu-Zr containing bulk amorphous alloys, Acta Materialia 54 (2006) 349-355.
[8] F. Szuecs, C.P. Kim, W.L. Johnson., Mechanical properties of $Zr_{56.2}Ti_{13.8}Nb_{5.0}Cu_{6.9}Ni_{5.6}Be_{12.5}$ ductile phase reinforced bulk metallic glass composite, Acta Materialia 49 (2001) 1507-1513.
[9] H. Choi-Yim, R.D. Conner, W.L. Johnson, Processing, microstructure and properties of bulk metallic glass composites, Annales de Chimie Science des Materiaux 27/5 (2002) 113-118 (in French).
[10] H. Tan, Y. Zhang, Y. Li, Synthesis of La-based in-situ bulk metallic glass matrix composite, Intermetallics 10 (2002) 1203-1205.
[11] Q. Wang, J.-J. Balandin, M. Suery, B. Van de Moortele, J.-M. Pelletier, High temperature deformation of a fully amorphous and partially crystallized bulk metallic glass, Annales de Chimie Science des Materiaux 27/5 (2002) 19-24.
[12] X. Hu, S.C. Ng, Y.P. Feng, Y. Li, Glass forming ability and in-situ composite formation in Pd-based bulk metallic glasses, Acta Materialia 51 (2003) 561-572.
[13] J. Eckert, U. Kühn, N. Mattern, G. He, A. Gebert, Structural bulk metallic glasses with different length-scale of constituent phases, Intermetallics 10 (2002) 1183-1190 .
[14] T.C. Hufnagel, C. Fan, R.T. Ott, J. Li, S. Brennan, Controlling shear band behaviour in metallic glasses through microstructural design, Intermetallics 10 (2002) 1163-1166.
[15] N. Mattern, Structure formation in Metallic Glasses, Kolloquium "Microstructure Analysis in the Materials Science", 56, Freiberg, 2005.
[16] N. Mattern, U. Kuehn, A. Gebert, T. Gemming, M. Zinkevich, H. Wendrock, et al., Microstructure and thermal behaviour of two-phase amorphous Ni-Nb-Y alloy, Scripta Materialia 53/3 (2005) 271-274.

[17] W.C.Wang, J.H. Li, F. Zeng, Y.L. Gu, B.X. Liu, Fractal morphologies of dual amorphous phases observed in Y-Ti(Nb)-Co ternary systems upon ion beam mixing, Journal of Alloys and Compounds 478 (2009) L28-L32.
[18] http://www-db1.imr.tohoku.ac.jp/java_applet/Amor_Ternary/amorphous_ternary.html
[19] P. Villars, A. Prince, H. Okamoto, Handbook of Ternary Phase Diagrams, ASM International, 1995.
[20] F. R. Boer, R. Boom, W.C.M. Mattens, A.R. Miedema, A.K. Niessen, Cohesion and structure. Cohesion in metals, vol. 1,: Elsevier Science, Amsterdam,1988.
[21] V.T. Witusiewicz, Thermodynamics of liquid binary alloys of the 3d transition metals with metalloids: Generalization, Journal of Alloys and Compounds 221 (1995) 74-85.
[22] A.A. Kundig, M. Ohnuma, D.H. Ping, T. Ohkubo, K. Hono, In situ formed two-phase metallic glass with surface fractal microstructure, Acta Materialia 52 (2004) 2441-2448.
[23] T. Kozieł, Z. Kędzierski, A. Zielińska-Lipiec, J. Latuch, Journal of Microscopy, TEM studies of the melt-spun alloys with liquid miscibility gap, (in press).
[24] J.H. Perepezko, G. Wilde, Amorphization and alloy metastability in undercooled systems, Journal of Non-Crystalline Solids 274 (2000) 271-281.
[25] M.H. Braga, J. Vizdal, A. Kroupa, J. Ferriera, D. Soares, L.F. Malheiros, The experimental study of the Bi–Sn, Bi–Zn and Bi–Sn–Zn systems, Computer Coupling of Phase Diagrams and Thermochemistry 31 (2007) 468-478.